International Journal of Applied Mathematics
& Statistical Sciences (IJAMSS)
ISSN(P): 2319-3972; ISSN(E): 2319-3980
Vol. 3, Issue 3, May 2014, 53-62

International Academy of Science, Engineering and Technology
Connecting Researchers; Nurturing Innovations

GROWTH, MORPHOLOGICAL, OPTICAL AND PHYSICAL PROPERTY STUDIES ON NONLINEAR OPTICAL SINGLE CRYSTALS OF MMTD

S. CYNTHIA[1], A. VICTOR ANTHONY RAJ[2], P. SAGAYARAJ[3] & B. MILTON BOAZ[4]

[1,2,3]Department of Physics, Loyola College, Chennai, Tamil Nadu, India

[4]Department of Physics, Presidency College, Chennai, Tamil Nadu, India

ABSTRACT

Nonlinear optical metal organic single crystal of Manganese Mercury Thiocyanate dimethylsulphoxide (MMTD) was grown by slow evaporation technique in aqueous solution. The crystal system and lattice parameters were determined by single crystal X-ray diffraction. FESEM analysis reveals that the surface of the crystal has minor defects and few dislocations. Atomic force microscopy shows that the crystal almost possesses a smooth surface. Energy dispersive X ray analysis confirm the chemical composition of the crystal in weight percentage. FTIR studies confirm the functional groups and formation of the crystalline compound. Kurtz and Perry powder technique confirm the SHG efficiency of MMTD. Epifluorescence studies reveal that the compound shows emission spectra with green fluorescence at 540 nm. Detailed dielectric measurements have been carried out and the dielectric constant was calculated. Photoconductivity studies reveal the photoconducting nature of the sample and the thermal stability was investigated by thermogravimetric analysis.

KEYWORDS: Organometallic, Photoconductivity, X-ray Diffraction, Atomic Force Microscopy

1. INTRODUCTION

Nonlinear optical (NLO) single crystals with their unique properties have promising applications in the area of photonics such as high speed information processing, frequency conversion, optical communication, high optical disk data storage, etc., based on the idea of combining the inorganic distorted polyhedron with asymmetric conjugate organic molecules. Organic class of crystals have been proposed as a new approach for the materials with interesting nonlinear optical properties for technologically important devices due to their physical, chemical and mechanical stability [1.2]. The semi-organic nonlinear optical (NLO) crystals have also been given a great deal of interest due to their superior properties such as high susceptibility, faster response, capability of designing components on the molecular level and large NLO co-efficient over the corresponding inorganic counterparts [3,4]. Hence, organometallic compounds have attracted a great deal of attention in the NLO field for opto-electronic devices. Among the different varieties of NLO materials investigated, the recent interest has been mainly focused on organometallic compounds due to their unique charge transfer capability associated with charge transfer transitions either from metal to ligand or ligand to metal [5]. The metal ligand bonding in organometallics give rise to large molecular hyper-polarizabilities by the transfer of electron density between the metal atom and the conjugated ligand systems [6].

Ligand like thiocyanate (SCN) with S and N donors is capable of combining with metal to form stable complexes through coordinated bonds. The crystals formed with SCN ligand have shown a relatively higher SHG effect than those crystals formed with the other organic ligands. However like organic materials, organometallic compounds also offer the advantages of architectural flexibility and ease of fabrication [7, 8]. The grown MMTD crystals are subjected to single

crystal X-ray analysis, Field emission scanning electron microscopy (FESEM), Atomic force microscopy (AFM), Fourier transform infrared analysis (FTIR), Epifluorescence studies, Thermogravimetric and differential thermal analysis (TGA/DTA), Photoconductivity studies and Dielectric property measurements. The NLO activity was also performed by Kurtz and Perry technique.

2. EXPERIMENTAL PROCEDURE

All starting materials were analytical reagent grade (purity ≥98.0%) and used as purchased, and all synthesis and growth processes were carried out in aqueous solution. Manganese Mercury Thiocyanate (MMTC) and its lewis base adduct Manganese Mercury Thiocyanate dimethylsulphoxide (MMTD) was synthesized by taking ammonium thiocyanate, mercury chloride and manganese chloride in the stoichiometric ratio of 3:1:1. The raw materials used were synthesized in deionized water and stirred continuously using magnetic stirrer for over 5 hours until the salt is dissolved completely. The following reaction was observed during the process.

$$4NH_4SCN+MnCl_2+HgCl_2 \rightarrow MnHg(SCN)_4+4NH_4Cl$$

For synthesizing manganese mercury thiocyanate dimethylsulfoxide (MMTD), first MMTC crystals were crushed and the powder was dissolved in mixed solvent of DMSO and deionized water in the ratio 1:3. The following chemical reaction takes place during the process.

$$MnHg(SCN)_4 + 2C_2H_6OS \rightarrow MnHg(SCN)_4(C_2H_6OS)_2$$

As carried out in the preparation of MMTC crystal, the pH of the MMTD solution was also adjusted to be 3.4. In the case of MMTC, nucleation started after two weeks whereas, tiny MMTD crystals can be seen within a week after the solution was kept for evaporation. Defect free seed crystal chosen for further growth were hung with nylon thread and carefully suspended into the beaker containing super saturated solution and the solvent was allowed to evaporate at ambient temperature. As the solution evaporates progressively in constant temperature bath systems, good quality single crystals of MMTD were obtained within a period of 30 to 33 days. The photograph of the grown single crystals are shown in Figure 1.

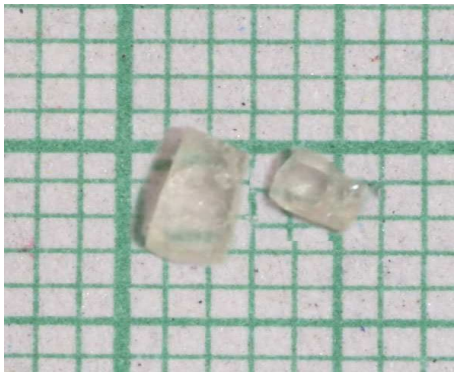

Figure 1: Photograph of as Grown MMTD Single Crystals

3. RESULTS AND DISCUSSIONS

3.1 Single Crystal XRD and Determination of Fundamental Parameters

The single crystal X-ray analysis of MMTD crystal was recorded using X-ray diffractometer (ENRAF NONIUS CAD4). The unit cell parameters a = 11.29 **Å**, b = 11.29 **Å**, c = 4.27**Å**, V = 544.2 $Å^3$ evaluated from the

single crystal X-ray analysis is in good agreement with the reported value [9]. The study also reveals that the space group of the crystal is P2121. The calculated value of the molecular density of the grown crystal was found to be ρ=2.523 g cm^{-3} and the valence electron plasma energy $\hbar\omega_p$ is given by,

$$\hbar\omega_p = 28.8 \left(\frac{Z\rho}{M}\right)^{1/2} \quad [1]$$

Where, z is the total number of valence electrons, ρ the density and M the molecular weight of MMTD crystal. The explicit factors depending on $\hbar\omega_p$ are the Penn gap $E_p$and the Fermi energy E_F given by the relations,

$$E_p = \frac{\hbar\omega_p}{(\varepsilon_r - 1)^{1/2}} \quad [2]$$

$$E_F = 0.2948(\hbar\omega p)^{4/3} \quad [3]$$

The molecular polarizability $\propto$ was obtained using the relation [10]

$$\propto = \left[\frac{(\hbar\omega_p)^2 S_0}{(\hbar\omega_p)^2 S_0 + 3E_p^2}\right] \times \frac{M}{\rho} \times 0.396 \times 10^{-24} \text{ cm}^{-1}$$

Where,

$$S_0 = 1 - \left[\frac{E_p}{4E_F}\right] + \frac{1}{3}\left[\frac{E_p}{4E_F}\right]^2 \quad [4]$$

The value of $\propto$ of the crystal so obtained is agreed well with the Clausious-Mossotti relation,

$$\propto = \frac{3M}{4\pi N_a}\frac{(\varepsilon_r - 1)}{(\varepsilon_r + 2)} \quad [5]$$

Where the symbols have their usual significance and N_a is the Avogadro number. The calculated fundamental parameters from single crystal XRD data of the grown MMTD crystal are presented in Table 1.

Table 1: Fundamental Parameters of MMTD Crystal Obtained at Room Temperature

Plasma Energy /eV	Penn Gap /eV	Fermi Energy /eV	Polarizability/cm^2	
			Penn Analysis	Clausious Mossotti
14.326	3.239	26.847	56.754*x10*$^{-24}$	51.413*x10*$^{-24}$

3.2 FESEM Analysis

FESEM analysis was carried out using Field Emission Scanning Electron Microscope in order to analyze the nature and surface morphology of the grown MMTD crystal. The crystal was cut into few mm for observing the surface morphology and the FESEM images of MMTD crystal are taken in three different magnifications as depicted in Figure 2. The images clearly establish the step-like growth, which suggests the existence of grain boundaries and striations. In consequence of the same it is predicted that the surface is smooth and free from any visible inclusions. The micrographs also show the presence of few cracks on the crystal surface which may be due to the temperature oscillations during the crystal growth. Figure 2a shows the formation of nano crystals and the growth pattern was uniform and homogenous whereas in Figure 2b the changes on the surfaces and the patterns were due to the optimization of pH and temperature. Figure 2c shows that the crystal surface contains regular voids and are cubic in nature. Dendrite growth pattern and formation of minute crystallites over the surface were also observed [11].

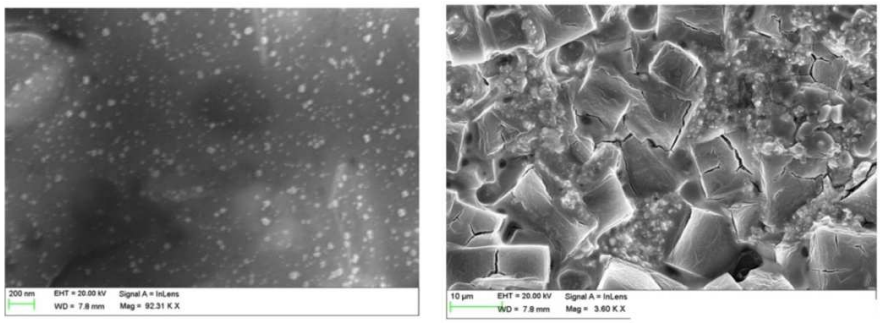

(a) **(b)**

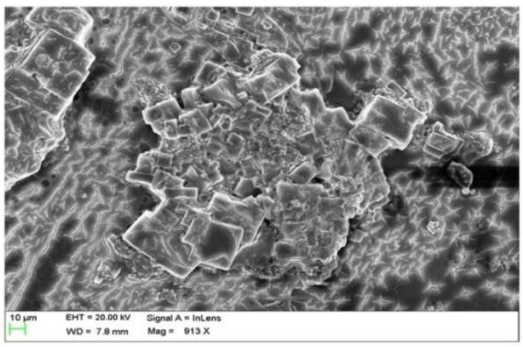

(c)

Figure 2: FESEM Images of MMTD Crystal

3.3 AFM Amplitude Analysis

To collect the three dimensional image for MMTD crystal, NT-MDT, NTEGRA PRIMA – Modular AFM was used. Atomic force microscopy (AFM) is an advanced technique, for observing crystal growth dynamics as well as imaging and computing surface features on a nanometer resolution. The amplitude parameters of a sample are described by the parameters which give information about statistical average values, shape of the histogram heights and other extreme properties [12].

The average roughness (Sa) is the mean height as calculated over the entire measured length/area. Root mean square (RMS) roughness (Sq) is the square root of the distribution of surface height and is considered to be more sensitive than the average roughness. Ten-point mean height roughness (Sz) is the difference in height between the average of five highest peaks and five lowest valleys in the evaluation profile/surface and is more sensitive to occasional high peaks or deep valleys than Sa. Surface skewness (Ssk) is used to measure the symmetry of the variations of a profile/surface about the mean line/plane. Coefficient of kurtosis (Sku) is used to measure the distribution of the spikes above and below the mean line/plane. The values of the same are presented in Table 2. The results of skewness and kurtosis obtained from the Figure 3 show that the crystal surface is spiky with dominant peaks. The micrographs reveal that the surface is indicative of a crack free and pinhole free surface together with the related size distribution analysis, based on Gaussian functions. In fact, the size of the histograms showed that, during the growth, the mean diameter increased together with an impressive change in the distribution width of the material. This behaviour can be explained considering that the crystal growth is controlled by surface processes [13]. Figure 4 shows the two-dimensional AFM micrograph where, the grain distribution is uniform. The grain size increases with increase in the thickness of the surface which is due to larger ionic radius of Mn causing larger clumps of unit cells or grains [12].

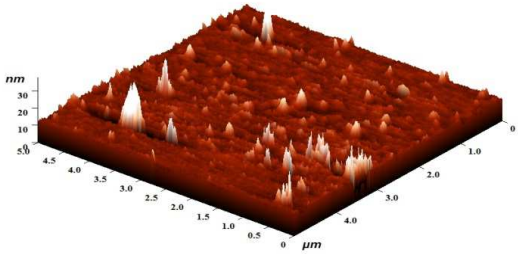

Figure 3: Three Dimensional Image of MMTD Crystal

Table 2: Roughness Parameters of MMTD

Peak-to-peak, Sy	23.4415 nm
Ten point height, Sz	11.1161 nm
Average	4.13662 nm
Average Roughness, Sa	0.428618 nm
Root Mean Square, Sq	0.918211 nm
Surface skewness, Ssk	7.62499
Coefficient of kurtosis, Sku	108.827

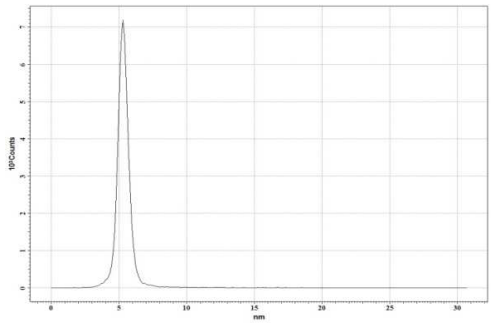

Histogram Peak

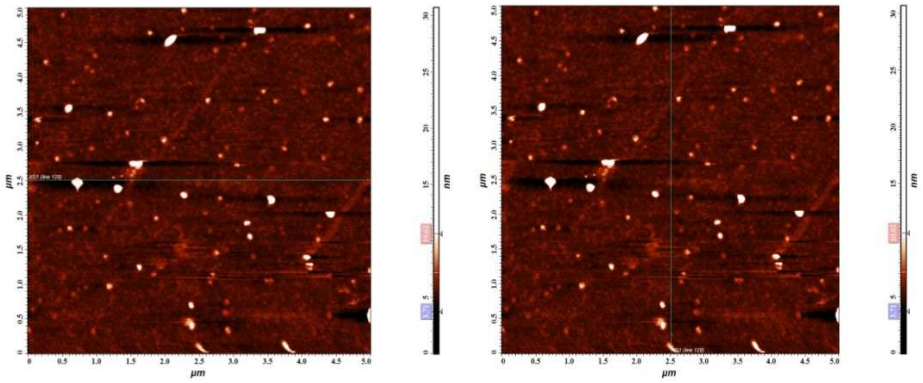

Horizontal Cross Section **Vertical Cross Section**

Figure 4: Two Dimensional AFM Micrographs of MMTD Single Crystal

3.4 Energy Dispersive X-ray Analysis

Energy dispersive X-ray analysis (EDAX) is a micro-analytical technique, used to obtain information about the chemical composition of the grown crystal. The grown crystal was subjected to EDAX analysis using the instrument supra 55 coupled with Carl Zeiss and bombarded with 20,000 volts and the obtained EDAX spectrum of the crystal is shown in Figure 5. The spectrum confirms the exact chemical composition of MMTD. The various elements present in MMTD with weight percentage and atomic percentage is presented in Table 3.

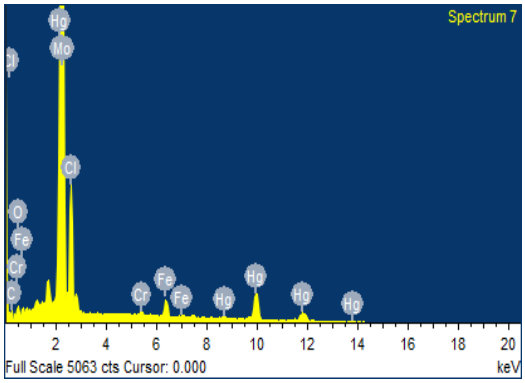

Figure 5: EDAX Spectrum of MMTD Crystal

Table 3: EDAX Analysis of MMTD Crystal

Element	Weight %	Atomic %
C K	5.86	31.60
O K	2.50	10.11
Cl K	11.98	21.91
Cr K	0.54	0.67
Fe K	3.69	4.28
Ni K	0.58	0.64
Mo L	18.72	12.65
Hg M	56.14	18.14
Totals	100.00	

3.5 Fourier Transform Infrared (FTIR) Analysis

The FTIR analysis of MMTD single crystal was carried out using KBr pellet technique by IFS BRUKER 66V FTIR spectrometer to confirm the functional groups and formation of the crystalline compound and the spectrum obtained is shown in Figure 6. In the FTIR spectrum of MMTD the intense sharp peak at 2112 cm^{-1} is assigned to CN vibrations. The CS vibration is observed to produce a less intense peak at 773 cm^{-1}. The peaks at 441 cm^{-1} and 914 cm^{-1} are due to the bending modes of NCS. In the higher energy region of the spectrum, OH vibrations of H_2O produce more intense broad band at 3319 cm^{-1}. The bending mode of water is seen at 1696 cm^{-1}. The frequency assignments of MMTD in the present study are presented in Table 4. The assignment of the main characteristic IR band frequency is in good agreement with literature [14]

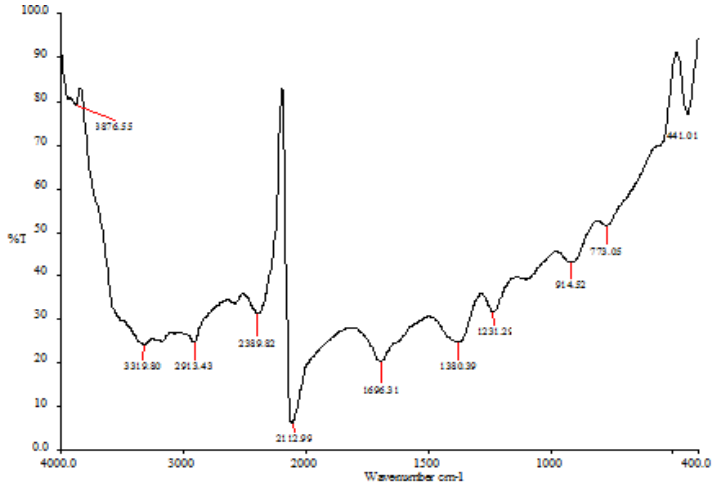

Figure 6: FTIR Spectrum of MMTD Crystal

Table 4: Frequency Assignments of IR Band Frequencies Observed for MMTD

Band Frequencies for MMTD Crystal (cm^{-1})	Assignment
2112	CN stretching
773	CS vibration
441	NCS bending
914	NCS bending
3319	OH vibration
1696	H_2O stretching
1231	C- H bending

3.6 Second Order NLO Test

The second harmonic generation efficiency of MMTD has been studied using Kurtz and Perry technique [15]. The sample was tested using Q switched Nd: YAG laser beam of wavelength 1064 nm, Quanta ray series supplied by spectra Physics and Coherent molectron power meter. An input power of 6.8 mJ/pulse and pulse width of 8 ns with a repetition rate of 10 Hz was used. The grown crystals were crushed into a fine powder and then packed in a micro capillary of uniform bore and exposed to laser radiations. The 532 nm radiation was collected by a monochromator after separating the 1064 nm pump beam with an Infra-red blocking filter. Second harmonic radiation generated by the randomly oriented micro crystals was focused by a lens and detected by a photo multiplier tube. The emission of green light confirms the second harmonic generation property of the crystal. Comparison of the SHG output of MMTD with the standard NLO crystal KDP reveal that the SHG efficiency of MMTD is 1.3 times that of KDP and this agrees well with the earlier report [16].

3.7 Epifluorescence Analysis

An optical study was performed by means of Bright field/ Fluorescence microscopy (Nikon Eclipse 80i). Fluorescence is a molecular phenomenon in which a substance absorbs light of some colour and almost instantaneously radiates light of another colour with lower energy and thus longer wavelength. This process is known as *excitation* and *emission*. The most important advance in fluorescence microscopy was the development of episcopic illumination for fluorescence microscopes in 1929. The first Epifluorescence microscope probably used half-silvered mirrors for the beam splitter, with a maximum overall efficiency of 25%. Fluorescence may be expected generally in molecules that are aromatic or contain multiple conjugated double bonds with a high degree of resonance stability [17]. Fluorescence finds wide application in the branches of biochemical, medical, and chemical research fields and also used as lighting in fluorescent lamps, LED etc. The Epifluorescence emission spectrum for MMTD was recorded in the wavelength range 400 – 700 nm. It is observed from the fluorescent image that the compound shows complete emission. Hence MMTD possess green fluorescence at 540 nm as shown in Figure 7.

Figure 7: Epifluorescence Image of MMTD Crystal

3.8 Dielectric Studies

The dielectric constant and the dielectric loss of MMTD crystals were measured along the growth plane (100) at a room temperature using HIOKI 3532 LCR HITESTER in the frequency range 50 Hz to 5 MHz. Figure 8 shows the plot of dielectric constant ϵ_r versus log frequency. It is observed from the profile that the dielectric constant has high values in the lower frequency region and then decreases with the applied frequency of MMTD. The very high value of ϵ_r at low frequencies may be due to the presence of all the four polarizations namely, space charge, orientation, electronic and ionic polarization and its low value at higher frequencies may be due to the loss of significance of these polarizations gradually. The low value of dielectric constant at high frequency testifies the optical quality of the crystal [18].

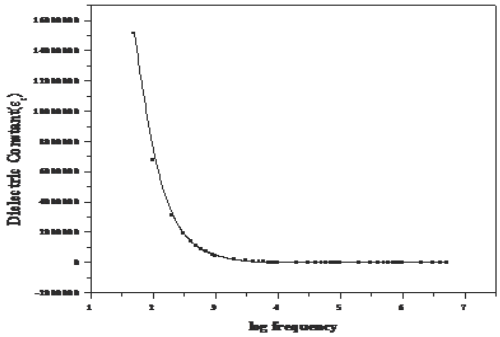

Figure 8: Dielectric Constant vs Log Frequency of MMTD Crystal

3.9 Photoconductivity Measurements

The measurements of photocurrent and dark current of MMTD were done using the Picoammeter (Keithley 480). The dark current was recorded by keeping the sample unexposed to any radiation. Figure 9 shows the variation of both dark and photocurrent with applied field at different levels of illumination. The required current is noted for variation. It is seen from the plots that both dark and photocurrent of the sample increase linearly with the applied field and the dark current is less than photocurrent at any instant for the same applied field. The photoconductivity exhibited by the sample may be due to the reduction in the number of charge carriers in the presence of radiation. According to the Stockmann model, photoconductivity is based on two level-scheme. One level is located between the Fermi level and the conduction band, while the other is close to the valence band. The second state has high capture cross sections for electrons and holes. Thus the net number of mobile charge carriers is reduced due to incident radiation. This may be due to more positive charge of manganese and mercury metal ions [19].

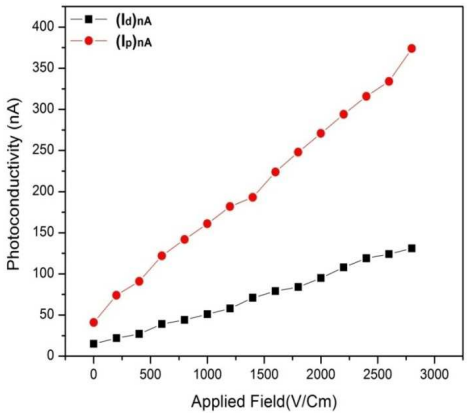

Figure 9: Photoconductivity Nature of MMTD Crystal

3.10 Thermal Analysis

A ceramic crucible was employed for heating the sample and the analysis was carried out using Perkin Thermal Analyser in an atmosphere of nitrogen at a heating rate of 20 ˚C /min in the temperature range 50-875 ˚C. The TGA/DTA spectrum of MMTD exhibits three stages of weight loss. The first stage is between 220˚C to 430˚C and the second stage is from 430˚C to 690˚C then the final stage of weight loss occurred between 690˚ to 875˚C. It is pertained to know that no decomposition of the sample takes place till 220˚C. A careful examination of thermograph reveals the appearance of an endothermic peak around 390˚C in DTA trace depicted in Figure 10 signifies the melting point of the material [20].

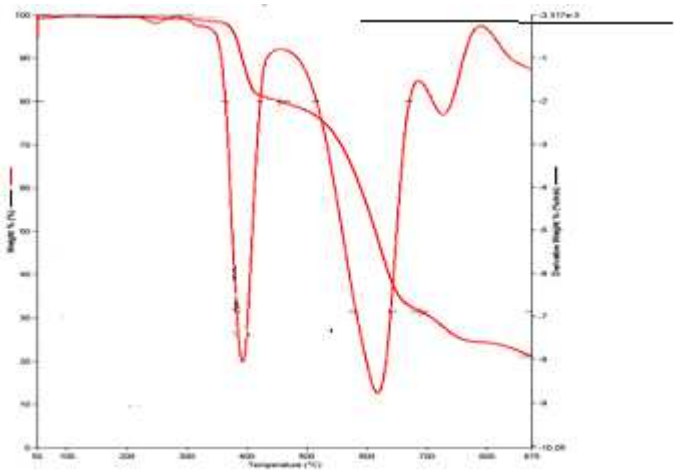

Figure 10: TGA/DTA Spectrum of MMTD Crystal

4. CONCLUSIONS

Good quality organometallic compound MMTD single crystal was grown by slow evaporation method within a period of 33 days. Identification of the crystal was confirmed by XRD analysis. The FESEM study shows that the crystal contains smooth surface with few minute crystallites and dendrite growth patterns. Atomic Force microscopy analysis shows that the crystal surface is spiky with dominant peaks. Energy dispersive X ray analysis confirm the chemical composition of the crystal in weight percentage. The functional groups and formation of the compound are confirmed by FTIR analysis. The NLO efficiency of the crystal was estimated by Kurtz and Perry technique. Epifluorescence image reveal that the sample was excited at 540 nm. The frequency dependence of dielectric constant increases with decreasing frequency at a particular temperature. Photoconductivity study reveals that the photocurrent is greater than the dark current at varying fields. The thermal behavior of the grown crystal studied by TGA/DTA reveal the thermal stability of the sample.

REFERENCES

1. M.D. Agarwal, J. Stephens, A.K. Batra, R.B. Lal, J. Optoelectronics Adv. Mat., 5 (2003) 555.
2. S. Debrus, H. Ratajczak, J. Venturini, N. Pincon, J. Baran, J. Barycki, T. Glowiak, A. Pietraszko, Synth. Met., 99 (2002) 127.
3. R. Sankar, C.M. Raghavan, R. Mohan Kumar, R. Jayavel, J. Cryst. Growth., 30 (2007) 309.
4. B. Milton Boaz, J. Mary Linet, B. Varghese, M. Palanichamy, S. Jerome Das, J. Cryst. Growth., 280 (2005) 448.

5. H.S. Nalwa, Appl. Organomet. Chem., 5 (1991) 349.
6. X.Q. Wang, D. Xu, M.K. Lo, D.R. Yuan, D.H. Zhang, F.Q.M.Q. Meng, S.Y. Guo, M. Zhou, J.R. Liu, X.R. Li, Cryst. Res. Techn., 36 (2001) 73.
7. Lu G.W, Xia H. R, Sun D.L, et al., Phy Status, Solidi, 231 (2002) 554.
8. Joseph G. P, Philip J. Rajarajan K, et al., J Cryst Growth, 51 (2006) 296.
9. Duan X. L, Yuan D.R, Wang X.Q, et al., J Cryst Res Techn., 10 (2002) 37.
10. N.M. Ravindra, V.S. Srivastava, Infrared Phys. 6 (1980) 20.
11. T. Rajesh Kumar, R. Jeyasakaran, S.M. Ravikumar, M. Vimalan, P. Sagayaraj., Appl Surf Sci, 257 (2010) 1687.
12. Ala'eddin A Saif, N. Ramli, P. Poopalan., Jordan J. Phy, 3 (2010) 63.
13. L. Latterini, L. Tarpani., Atomic Force Microscopy Investigations 7 (2012) 89.
14. Sethu Gunasekaran, Padmapriya Venkatesan, Govindarajulu Anand, Subramanian Kumaresan., Der Pharma Chemica, 4 (2012) 1111.
15. Kurtz S.K. and Perry T.T, J. Appl. Phys., 39 (1986) 3798.
16. Sethu Gunasekaran, Padmapriya Venkatesan, Govindarajulu Anand, Subramanian Kumaresan., Der Pharma Chemica, 4 (2012) 1111.
17. T. Uma Devi, N. Lawrence, R. Ramesh Babu, K. Ramamurthi, G. Bhagavannarayana., J. Min. Mat. Charac. Engg. 4 (2010) 328.
18. C. Balarew, R. Duhlew., J. Solid State Chem. 1 (1984) 55.
19. K. Rajarajan, S. Selvakumar, Gulam Mohammed, Vedha Potheher, P. Sagayaraj., Indian J Pure Appl Phy, 43 (2005) 930.
20. B. Uma, K Sakthi Murugesan, S. Krishnan, R. Jayavel, B. Milton Boaz., J. Mat. Chem. Phy., 142 (2013) 662.